J. Synchrotron Rad. (1998). **5**, 926–928

Multiple-wavelength powder diffraction using imaging plates at the Australian National Beamline

David J. Cookson, Brett A. Hunter, Shane J. Kennedy and Richard F. Garrett

Australian Nuclear Science and Technology Organisation, Private Mail Bag 1, Menai 2234, Australia. E-mail: m.webster@soton.ac.uk

(*Received 4 August 1997; accepted 12 November 1997*)

The Australian powder diffractometer at the Photon Factory is capable of recording multiple powder-diffraction scans in less than 5 min per pattern using imaging plates in Debye–Scherrer geometry. This, coupled with incrementing the X-ray beam energy in suitably small steps (down to ∼2 eV) between exposures, allows fast collection of anomalous diffraction data. Data collected from a copper oxide-based superconductor at energies near the Cu *K*-absorption edge are presented, along with an account of the technique used to extract multiple-exposure powder-diffraction data from imaging plates.

Keywords: imaging plates; X-ray powder diffraction; anomalous scattering; high-T_c superconductors.

1. Introduction

Rietveld analysis of powder-diffraction patterns is a well established technique for refining the structure of polycrystalline samples, but there are occasions when significantly different structure models can give equally good fits to the experimental data. Such a situation can occur when structures contain different atomic species with very similar numbers of electrons, resulting in similar X-ray scattering amplitudes.

In multiple anomalous powder-diffraction (MAPD) measurements, the coherent X-ray scattering power of a specific atom is adjusted by selecting incident energies close to the absorption edge of that atom (Will *et al.*, 1987; Attfield, 1990). This type of measurement can provide enough extra information to determine successfully a unique structure. Such an approach requires multiple sets of scattering data to be collected on the same sample at carefully calibrated energies with an error of less than 2 eV (Wilkinson *et al.*, 1991). Synchrotron radiation can provide high-intensity X-rays with continuously selectable energies, but the time available for collecting data on a single sample is necessarily limited due to the over-demand of such facilities. As a result, any improvement to time efficiency in multiple-wavelength measurements is desirable.

The main impediment to multiple-wavelength powder diffraction is the scanning time required for each sample. When collecting only two powder scans, the sample fluorescence (proportional to the absorption coefficient) can be used as a measure of the f'' component of the atomic scattering factor, from which the f' minimum energy can be inferred. Clearly, this has to be performed carefully to optimize the change in f', especially if each powder scan takes hours to complete. If a large number of powder scans can be collected at small energy intervals through the absorption-edge region, a good sampling of different f' values is assured. Wavelength and f' determinations can be performed at a later time, but, for this technique to be practical, the time taken to collect a complete powder pattern must be relatively short.

Imaging plates are becoming more widely used in synchrotron radiation facilities because of their high sensitivity, large dynamic range and high count rate (Amemiya *et al.*, 1988). These capabilities are well suited to powder diffraction, where the imaging plates can record an entire pattern in only a few minutes. High-pressure X-ray powder diffraction was one of the first XPD techniques to take advantage of the high sensitivity of imaging plates. Using a diamond pressure anvil, a single imaging plate could be used to record entire Debye rings (Nelmes *et al.*, 1992). Imaging plates have been employed more recently for XPD studies of dynamic gibbsite crystallization in hot caustic solutions (Gerson *et al.*, 1996). With the addition of a Weissenberg screen and a cassette that can translate the imaging plates, a complete set of multiwavelength strip exposures can be collected in a relatively short period of time. Such a set-up lends itself well to the measurement of powder samples at different temperatures (Espeau *et al.*, 1997)

2. Experimental

The Australian powder diffractometer (Barnea *et al.*, 1992; Garrett *et al.*, 1995), installed at beamline 20B at the Photon Factory, Japan, is a large-radius (573 mm) Debye–Scherrer camera. Diffracted intensities are obtained from up to eight imaging plates mounted on a translatable cassette. A Weissenberg screen allows multiple exposures to be rapidly accumulated as separate strips on a set of imaging plates (Fig. 1). The translation of the imaging plates with temperature, pressure or wavelength allows a series of diffraction patterns to be collected on the same sample with changing conditions. Typically 30 patterns can be collected on one set of imaging plates. A pixel resolution of (100 μm) obtained from scanning the exposed Fuji imaging plates in a BAS2000 imaging-plate scanner produces an effective resolution of 0.01° of arc in 2θ.

The monochromator used for wavelength selection is a water-cooled channel-cut Si(111) crystal mounted on a rotation stage. The angle of the monochromator crystal is monitored with a

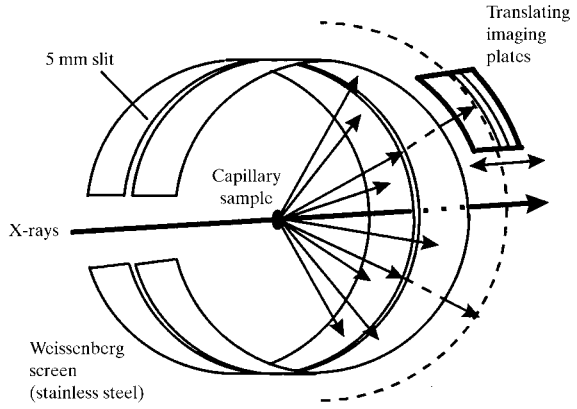

Figure 1
Schematic diagram of the Australian diffractometer in Debye–Scherrer mode using imaging plates and a Weissenberg screen.

Heidenhain angle encoder, allowing the monochromator angle to be measured with a precision of $\pm 0.0001^\circ$. This gives a precision in measuring energy of ± 0.05 eV in the 9 keV region.

The unique capabilities of the instrument allow a series of powder patterns to be collected over a range of energies close to the absorption edge of specific atom types. To illustrate this, we present here preliminary results from work on the $YBa_2Cu_3O_{6.95}$ superconductor (Hunter *et al.*, 1997) for which powder patterns were collected around the Cu *K*-edge. Other workers have already demonstrated the possibility of deriving site-resolved X-ray absorption-edge spectra from specific powder-diffraction lines of $YBa_2Cu_3O_x$ compounds (Attfield, 1991).

The $YBa_2Cu_3O_{6.95}$ sample was contained in a rotating 0.3 mm capillary. Four imaging plates were used to cover a 2θ range of 5–160°. Each powder pattern was obtained from a strip of exposed intensity running across all four imaging plates. Across each exposed strip the pixels were averaged normal to the scattering plane such that each point on the final powder pattern represented an average of between 30 and 50 pixels of intensity. This data-extraction technique contrasts other methods in which the intensities over entire Debye rings are integrated (Piltz *et al.*, 1992). Although our technique only integrates a small portion of the Debye ring, ample statistics are still obtainable for Rietveld analysis (Cookson *et al.*, 1996).

The Cu *K*-edge was found using the fluorescence from the sample and a series of powder-diffraction patterns collected at non-linear steps of energy around the Cu *K*-edge. The sequence of 31 exposures, ranging from approximately 800 eV below the Cu *K*-edge to 800 eV above, took less than 3 h.

The 2θ zero offset was calculated for each imaging plate using fiducial marks created by small radioactive sources embedded in the imaging-plate cassette. These gave an initial accuracy of $\pm 0.02^\circ$ for the offset which was later refined to an accuracy of $\pm 0.001^\circ$ in the Rietveld analysis. All the patterns collected were refined using the *LHPM* Rietveld package (Hill *et al.*, 1995) starting from known atomic coordinates and lattice parameters for the structure.

3. Results and discussion

Fig. 2 compares 13 powder patterns over a small 2θ angle range taken at energies close to the Cu $K\alpha$-absorption edge. In this region the energy increment between successive exposures ranged from 50 eV down to 1.6 eV. The patterns in this figure have had their backgrounds subtracted, hiding the dramatic change in the background resulting from fluorescence at energies greater than the absorption edge. This was performed to highlight the more subtle effect of passing through the f' minimum energy (shown by the f'_{min} arrow) which results in a gentle dip superimposed upon the larger slope caused by the change in X-ray absorption of the sample.

Fig. 3 shows the refined values of the f' atomic scattering factor for Cu at energies near the absorption edge from a $YBa_2Cu_3O_{6.95}$ sample (Hunter *et al.*, 1997). Values proportional to f' were obtained from the fluorescence and are also shown. At this point, further refinements to determine site occupancies were then successfully undertaken, and will be reported in later work.

It should be noted that, in spite of the fact that imaging plates are sensitive to fluorescence, the signal-to-noise ratio in the final powder patterns even after subtracting large backgrounds was excellent. This is illustrated by the fact that it is possible to see the first near-edge XAFS oscillation on the powder profile marked by the f''_{max} arrow in Fig. 2.

4. Conclusions

Using the sensitivity and high count rate of imaging plates, coupled with the capability to capture multiple exposures on one set of imaging plates, allows us to use a new method for efficiently performing multiwavelength anomalous powder diffraction. A wealth of data can be collected in a relatively short time, with only an approximate determination of the f' minimum energy (± 20 eV) required beforehand.

We acknowledge Dr Garry Foran for his assistance and support at the Australian beamline. This work was supported by the Australian Synchrotron Research Program which has been funded by the Commonwealth of Australia *via* the Major National Research Facilities Program.

References

Amemiya, Y., Matsushita, T., Nakagawa, A., Satow, Y., Miyahara, J. & Chikawa, J. (1988). *Nucl. Instrum. Methods*, A**266**, 645–653.
Attfield, J. P. (1990). *Nature (London)*, **343**, 46–49.
Attfield, J. P. (1991). *J. Phys. Chem. Solids*, **52**, 1243–1249.

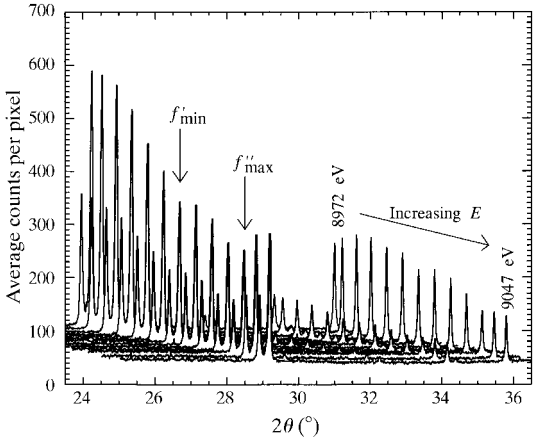

Figure 2
Multiple plot of powder-diffraction data from $YBa_2Cu_3O_{6.95}$.

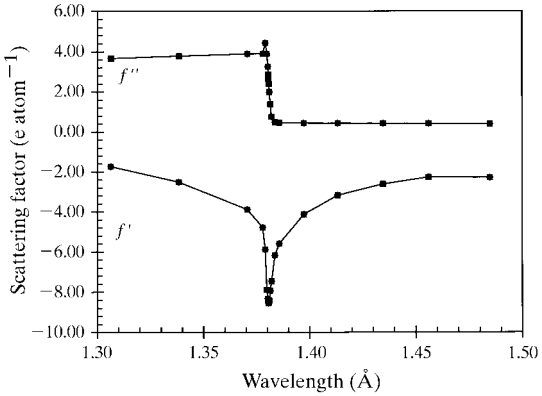

Figure 3
Atomic scattering factors (f' and f'') *versus* wavelength derived from $YBa_2Cu_3O_{6.95}$ powder-pattern refinements.

Barnea, Z., Creagh, D. C., Davis, T. J., Garrett, R. F., Janky, S., Stevenson, A. W. & Wilkins, S. W. (1992). *Rev. Sci. Instrum.* **63**, 1069–1072.
Cookson, D. J., Foran, G. J., Hunter, B. A., Ismunandar & Kennedy, B. J. (1996). *Mater. Sci. Forum*, pp. 228–331, 113–118.
Espeau, P., Reynolds, P. A., Dowling, T., Cookson, D. & White, J. W. (1997). *J. Chem. Soc. Faraday Trans.* **93**, 3201–3208.
Garrett, R. F., Cookson, D. J., Foran, G. J., Sabine, T. J., Kennedy, B. J. & Wilkinson, S. W. (1995). *Rev. Sci. Instrum.* **66**, 1351–1353.
Gerson, A. R., Counter, J. A. & Cookson, D. J. (1996). *J. Cryst. Growth*, **160**, 346–354.
Hill, R. J. & Howard, C. J. (1986). *LHPM. A Computer Program for Rietveld Analysis of Fixed-Wavelength X-ray and Neutron Powder Diffraction Patterns.* Report No. M112, Australian Nuclear Science and Technology Organization, Mail Bag 1, Menai 2234, Australia.
Hunter, B. A., Kennedy, S. J., Howard, C. J. & Cookson, D. J. (1997). Submitted for publication.
Nelmes, R. J., Hatton, P. D., McMahon, M. I., Piltz, R. O., Crain, J., Cernik, R. J. & Bushnell-Wye, G. (1992). *Rev. Sci. Instrum.* **63**, 1039–1042.
Piltz, R. O., McMahon, M. I., Crain, J., Hatton, P. D., Nelmes, R. J., Cernik, R. J. & Bushnell-Wye, G. (1992). *Rev. Sci. Instrum.* **63**, 700–703.
Wilkinson, A. P., Cox, D. E. & Cheetham, A. K. (1991). *J. Phys. Chem. Solids*, **52**, 1257–1266.
Will, G., Masciocchi, N., Hart, M. & Parrish, W. (1987). *Acta Cryst.* A**43**, 677–683.